OPTICAL AND ELECTRICAL INVESTIGATIONS INTO CATHODE IGNITION AND DIODE CLOSURE

J.J. Coogan, E.A. Rose, and R.P. Shurter

Los Alamos National Laboratory
Pulsed Power Systems Group, MS E525
Los Alamos, NM 87545

Abstract

A combination of optical and electrical diagnostics has been fielded on the Electron Beam Test Facility to study ignition and closure in large area electron beam diodes. A four-channel framing camera is used to observe the formation of microplasmas on the surface of the cathode and the subsequent movement of these plasmas toward the anode. Additionally, a perveance model is used to extract information about this plasma from voltage and current profiles. Results from the two diagnostics are compared. Closure velocity measurements are presented showing little dependance on applied magnetic field for both velvet and carbon felt emitters. We also report the first observation of the screening effect in large area cold cathode diodes.

Introduction

The temporal behavior of high-power diodes is closely related to the impedance collapse caused by the movement of the cathode and/or anode plasmas. This impedance collapse can be especially problematic when a constant power electron beam is required. This is the case for the very large area (square meters) diodes used to pump the amplifiers within the Aurora KrF laser system [1]. The electron beam technology development program at Los Alamos utilizes the Electron Beam Test Facility [2] (EGTF) to study diode physics in an attempt to better understand the basic phenomenology of ignition and closure. A combination of optical and electrical diagnostics has been fielded in a study of the formation and expansion of cathode plasmas.

In the standard model [3], microscopic surface features, or whiskers, on the cathode enhance the applied electric field and a stable field emission is initiated. The resulting currents quickly heat the whiskers through ohmic heating and the whisker tips explode. The individual microplasmas thus formed then expand and merge, creating a sheath that covers the entire surface of the cathode. The low work function of the plasma allows for efficient emission of electrons into the gap between the anode and cathode. The total current is then limited by space-charge effects.

The expansion of the cathode plasma does not stop once it has covered the emitting surface. The surface of the plasma continues to move out from the cathode toward the anode. This results in a collapse of the diode impedance as the effective electrode gap is reduced. Eventually the plasma front reaches the anode, shorting the diode, and no more power can be extracted. In large-area diodes, a magnetic field is often applied to counteract the pinching of the electron beam caused by its own magnetic field. Self- and applied fields add vectorially and the electrons follow the resultant field lines.

The perveance model of Parker [4] can be used to calculate the effective inter-electrode gap throughout the discharge. The total current, I, flowing across a space-charge limited diode is given by the familiar Child-Langmuir equations:

$$I = P * U^{3/2}, \text{ and } P = (k * A)/D^2 \quad (1)$$

where P is the perveance, U the voltage across the diode, D the effective gap, A the cathode emitting area and $k = 2.3 \times 10^{-6}$ amps/volt$^{3/2}$. Using measured voltage and current values, these equations can be solved for D(t). The gap changes with time and is modeled as $(d_o - V_c * t)$ where d_o is the initial distance between the anode and cathode surfaces and V_c is the expansion velocity of the cathode plasma, called the closure velocity.

Calculations have been performed at Los Alamos on both the Electron Gun Test Facility (EGTF) and Large Aperture Module (LAM) [5] and by others elsewhere. Typical values for V_c range from 1 to 6 cm/μs. These measurements have demonstrated that V_c remains fairly constant throughout the discharge.

For e-beam machines with a pulse width greater than 250-ns closure effects are significant. For a reasonable match to the pulse-power driving circuitry, anode-cathode gaps typically range from 3 to 10 cm. This places an absolute upper limit on the useful extraction time for any electron beam of around 5 μs. In practice, this limit is rarely approached as the impedance of the diode rapidly collapses because the effective gap decreases. This introduces severe stress, not only on the pulse-power system itself but also on the design of any support structures near the beam, such as the vacuum barrier between the diode and whatever target is being excited. The impedance collapse also forces either a substantial increase in current and/or decrease in voltage of the electron beam, which reduces the usefulness of the system. Closure rates have little effect on the performance of short pulse systems, but ignition delays and uniformity limit the efficacy of these devices because the ignition time is a substantial fraction of total pulse length and localized hot spots can be formed.

Experimental Setup

The EGTF produces a 400-keV electron beam with a pulse length of 0.2 to 2 μs. Current densities of 75 A/cm^2 can be produced from an emitting surface of around 200 cm^2. A tapped water resistor voltage divider and Rogowski coil are used to measure the bushing voltage and diode current. Voltage and current probe signals are digitized at a rate of 100 MHz and are processed using ASYST data acquisition software. Corrections are made for bushing inductance on the voltage waveform to better approximate the true cathode potential. Rogowski signals can be directly observed or integrated.

Two cathode geometries have been studied. A Chang profile [6] produces little unwanted edge emission but complicates both optical measurements and electrical modeling due to its curved shape. A planar emitter, of similar size, simplifies data analysis but is more susceptible to edge effects. Figure 1 shows the results of field calculations for both geometries performed with a Sun™ station and FLUX2D software. Radiachromic images of beam profiles show that careful assembly results in little or no halo effect using the planar emitter. Both velvet and carbon felt emitters have been installed on each of the cathodes.

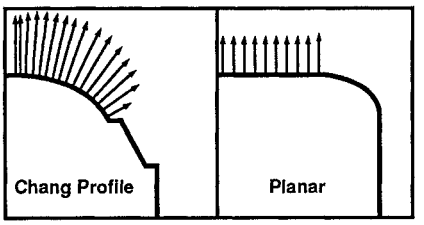

Fig. 1. Results of FLUX2D modeling of planar and Chang profile cathodes. The length of the arrows correspond to the surface field strength.

Report Documentation Page

Form Approved
OMB No. 0704-0188

1. REPORT DATE	2. REPORT TYPE	3. DATES COVERED
JUN 1991	**N/A**	**-**

4. TITLE AND SUBTITLE
Optical And Electrical Investigations Into Cathode Ignition And Diode Closure

5a. CONTRACT NUMBER
5b. GRANT NUMBER
5c. PROGRAM ELEMENT NUMBER

6. AUTHOR(S)

5d. PROJECT NUMBER
5e. TASK NUMBER
5f. WORK UNIT NUMBER

7. PERFORMING ORGANIZATION NAME(S) AND ADDRESS(ES)
Los Alamos National Laboratory Pulsed Power Systems Group, MS E525 Los Alamos, NM 87545

8. PERFORMING ORGANIZATION REPORT NUMBER

9. SPONSORING/MONITORING AGENCY NAME(S) AND ADDRESS(ES)

10. SPONSOR/MONITOR'S ACRONYM(S)
11. SPONSOR/MONITOR'S REPORT NUMBER(S)

12. DISTRIBUTION/AVAILABILITY STATEMENT
Approved for public release, distribution unlimited

13. SUPPLEMENTARY NOTES
See also ADM002371. 2013 IEEE Pulsed Power Conference, Digest of Technical Papers 1976-2013, and Abstracts of the 2013 IEEE International Conference on Plasma Science. Held in San Francisco, CA on 16-21 June 2013. U.S. Government or Federal Purpose Rights License.

14. ABSTRACT
A combination of optical and electrical diagnostics has been fielded on the Electron Beam Test Facility to study ignition and closure in large area electron beam diodes. A four-channel framing camera is used to observe the formation of microplasmas on the surface of the cathode and the subsequent movement of these plasmas toward the anode. Additionally, a perveance model is used to extract information about this plasma from voltage and current profiles. Results from the two diagnostics are compared. Closure velocity measurements are presented showing little dependance on applied magnetic field for both velvet and carbon felt emitters. We also report the first observation of the screening effect in large area cold cathode diodes.

15. SUBJECT TERMS

16. SECURITY CLASSIFICATION OF:			17. LIMITATION OF ABSTRACT	18. NUMBER OF PAGES	19a. NAME OF RESPONSIBLE PERSON
a. REPORT	b. ABSTRACT	c. THIS PAGE			
unclassified	**unclassified**	**unclassified**	**SAR**	**4**	

The four-channel framing camera , manufactured by EG&G is interfaced with a Stanford Research DG535 digital delay/pulse generator. Each channel is essentially a separate camera and the shutter time (5 - 100 ns), gain (up to 1000×), and trigger delay (0 ns – 0.99 s) can be set independently. The experimental setup is shown in Fig. 2. Viewports allow both side and front views of the cathode emitter. From the side, photographs show the expansion of a luminous plasma sheet from the cathode toward the anode. The time delays between exposures allow a straightforward calculation of the expansion velocity of the luminous front. The front view shows the spatial distribution of emitting sites on the surface of the cathode.

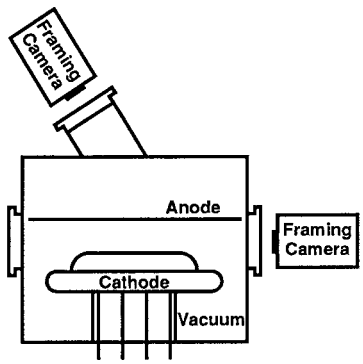

Fig. 2. Schematic showing arrangement of diode and diagnostics. Viewports allow framing camera photographs to be taken with side or front views of cathode.

Results

The perveance model of Parker can generate very useful measurements of the plasma motion within the diode and, if properly applied, the dynamics of e-beam transport. However, the two effects are difficult to decouple. Beam transport phenomenon such as emittance and beam pinching can be misinterpreted as simple closure effects. It must be remembered that in Eq. (1) not only do the voltage, current, and gap change with time but also the emitting area. For this reason we refer to the calculated gap as the effective gap.

Surface contamination can also affect measurements of closure velocity. Vacuum oil, grease, and any other substance on the surface of the cathode will be vaporized and produce additional plasma. The closure velocities measured just after reassembly are much larger than those on later shots. See Fig. 3. The impurities produce a substantial increase in closure velocities for all the cathode materials used.

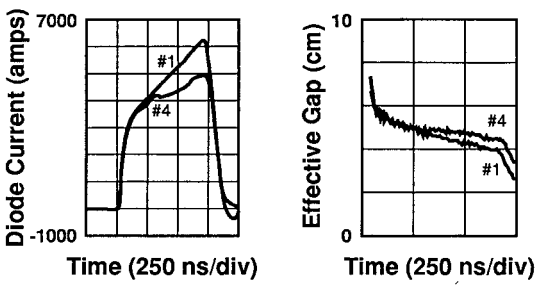

Fig. 3. Plot showing change in closure rates between first and fourth shot of day. (a) current (b) calculated effective gap.

Closure velocity calculations using the perveance model described above are consistent with earlier measurements when modest B-fields are applied [7,8]. Yet recent data, shown in Fig. 4, using both profiled and planar emitters show little if any dependance of applied B-field on closure velocities. The very low closure velocities reported in [8] for profiled emitters, with applied fields less than 1 kG, are not seen here. It is possible that beam transport effects are responsible for the lower values reported previously.

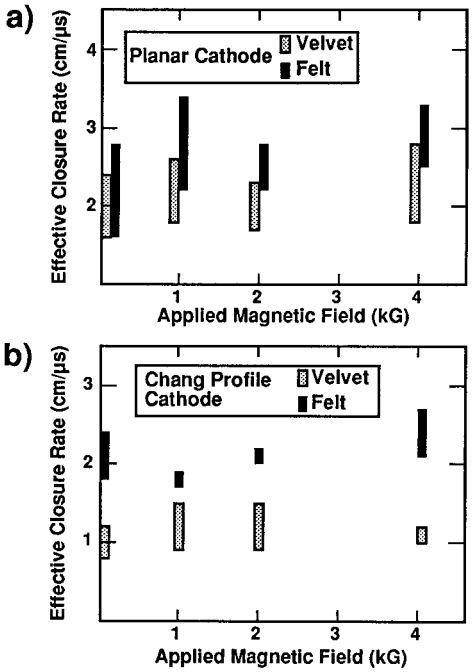

Fig. 4. Plots showing closure velocities as a function of applied B-field and cathode shape (a) planar cathode (b) Chang profile cathode.

Additional insight can be gained by comparing the predicted gap assuming an ideal emitter with that calculated from measured voltage and current waveforms. When the effective gap and a gap calculated assuming a uniform plasma covering the entire cathode and moving with a constant closure velocity are compared [9], the initial period of large effective gap is interpreted as the time required for the microplasmas to form a sheath over the cathode. This is referred to as the ignition time. Figure 5 compares the calculated effective gap for a Chang profile cathode with no applied B-field to the idealized D(t). The ignition time is around 100 ns. The divergence of the two lines near t+460 ns, not seen when a guide field is applied, is consistent with the onset of beam pinching. Although the plasma continues to expand toward the anode, the electron flow is constrained to a smaller cross-sectional area. The reduction in A in Eq. (1) results in an overestimation of the gap. In this work, the closure velocity is derived from a linear fit to the data points before the effects of beam pinch are observed.

More subtle effects of plasma expansion and/or beam transport have been observed with velvet emitters. Two types of velvet, one a loose knit the other very dense, were tested. The resulting effective gaps are shown in Fig. 6. Although the closure rates of these diodes are similar, the intercepts are significantly different. For the dense weave the effective gap extrapolates back to the expected value, d_0. The open weave yields a smaller intercept. One possible explanation is suggested by theoretical studies [10] showing that surface roughness has a substantial effect on beam emittance. The coarser surface of the open weave may result in a larger effective emitting surface, which would allow more current to flow. An increase in emitting area of only 10% would account for the additional current.

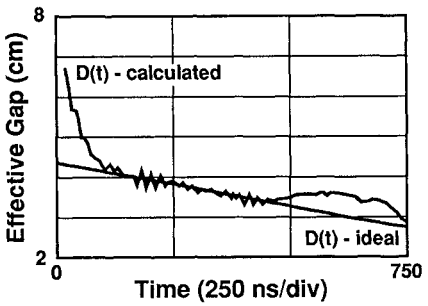

Fig. 5. Plot showing the calculated effective gap using a Chang profile cathode with no applied field. The effect of beam pinching can be observed.

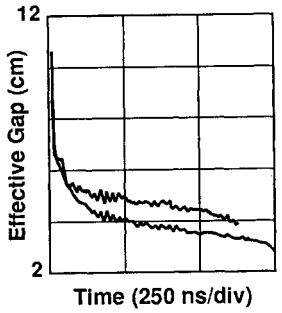

Fig. 6. Plot showing effect of surface structure on effective gap for two types of velvet.

Photographs obtained with a 40-ns framing speed are shown in Fig. 7. The view is from the side with the cathode below and the anode above. Closure velocities are obtained by measuring the width of the luminous bands at several time delays. A summary of the data obtained using both optical and electrical diagnostics is shown in Fig. 8.

Optical measurements yield overall closure velocities lower than electrical measurements. In this work agreement was observed early in the pulse between optical and electrical measurements as has been seen in short pulse systems [4]. The divergence, at later times, between optical and electrical closure rates can be explained in several ways. First, if the plasma expanded so that its density near the emitting surface was much lower than that near the cathode, the fluorescence intensity could be below the capabilities of the camera. Secondly, the plasma species present near the emitting surface may be different than those near the cathode and their fluorescence may not be within the spectral range of the camera. In aluminum multi-cathode-spot vacuum arcs, differences in the population of first and second ionization levels have been observed to change as a function of distance from the cathode [11]. And thirdly, the plasma expansion rate could change with time. More accurate and sensitive techniques, such as Planar Laser Induced Fluorescence [12] (PLIF), should be able to resolve these uncertainties.

Photographs of the front surface of the cathode are shown in Fig. 9. The number of spots is observed to increase, and thus the current per spot decrease, as the applied B-field is increased. This is consistent with the screening effect [3,13] observed in cylindrical, magnetically insulated diodes. In these systems, it was demonstrated that the space charge originating from an emission site decreased the electric field at the nearby cathode surface, retarding the formation of new emission sites. R_s can be calculated using a simple non-relativistic model [3]:

$$R_s = 500\ (V^{-0.75}\ i^{0.5}\ d_o)\ , \qquad (2)$$

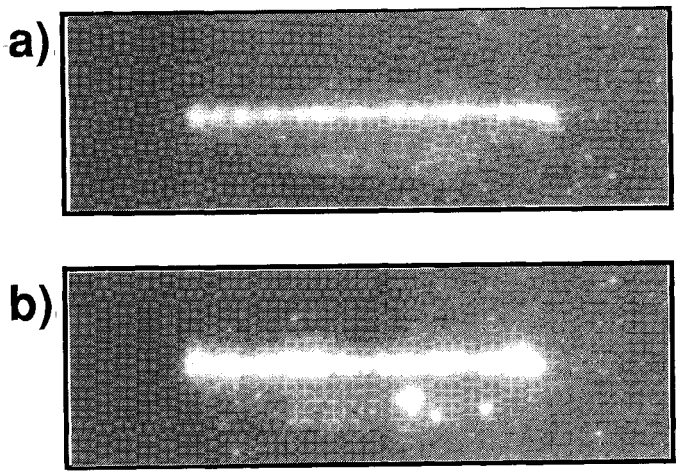

Fig. 7. Photographs of cathode plasma using a velvet emitter. The view is from the side, the shutter time 40 ns and the anode above the cathode. Delays of (a) 200 ns, (b) 600 ns. The several small spots in b are arcs near the cathode surround.

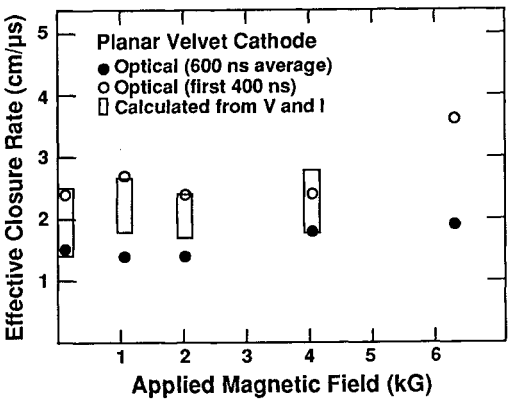

Fig. 8. Comparison of closure rates, calculated using measured electrical waveforms and time resolved photography.

where i is the current per emission site. The theory also predicted that as a guide magnetic field is applied there would be a decrease in the screening radius, R_s, as the gyroradii of emitted electrons are constrained by the B-field. The effect is reduced as the gyroradius approaches $V_c t$, and is therefore most pronounced at low magnetic fields.

Photographs of velvet emitters confirm this prediction on broad area cathodes. As the B-field is increased the spot density on the cathode surface is increased. Figure 10 shows a plot of the range of current/spot as a function of B-field during the first 300 ns of the pulse.

The number of cathode spots observed on the EGTF closely follows the current as shown in Fig. 11. The solid points correspond to the expected current given a constant value of 10 amps/spot. For i = 10 amps, V = 360 kV, d_o = 5.4 cm, R_s is approximately 0.6 cm. Increasing i to 14 amps, R_s is increased to 0.7 cm. The average spacing between emission sites in the data recorded in Fig. 9 varies from 0.9 to 0.7 cm as the B-field is increased from 0.5 to 4 kG. The gyroradius is greater than $V_c t$ throughout the pulse at 500 and 1 kG, and equal to $V_c t$ around 375 ns at 2 kG. This may explain the divergence of the last point in Fig. 11.

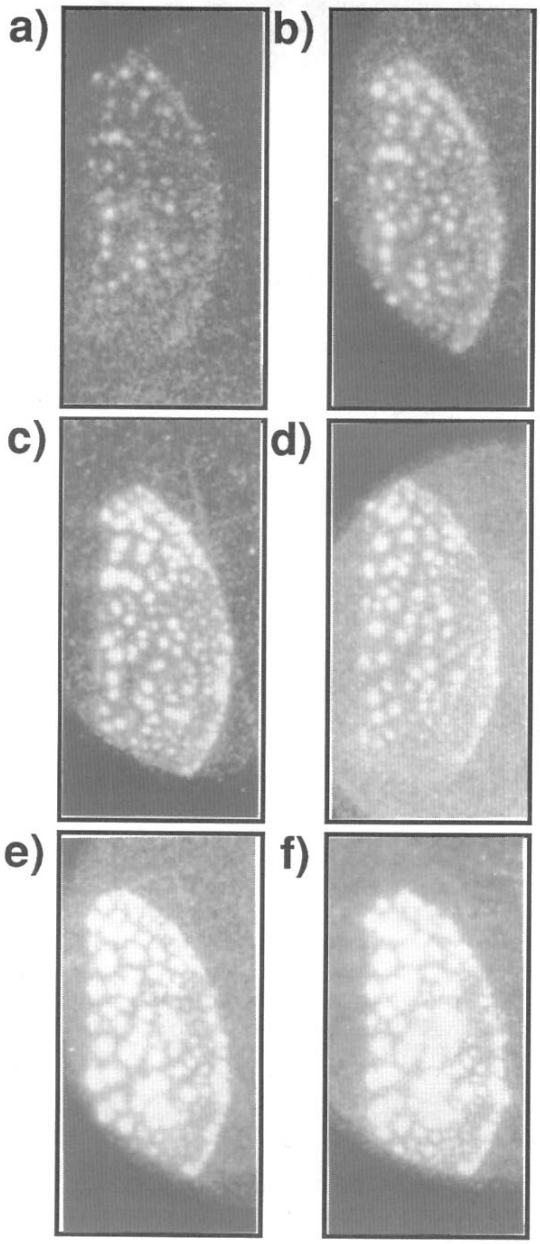

Fig. 9. Photographs of cathode plasma using a velvet emitter. The view is from the front, the shutter time 50 ns. Delays of (a) 50 ns (b) 100 ns (c) 150 ns, and (d) 150 ns (e) 350 ns (f) 750 ns on two successive shots.

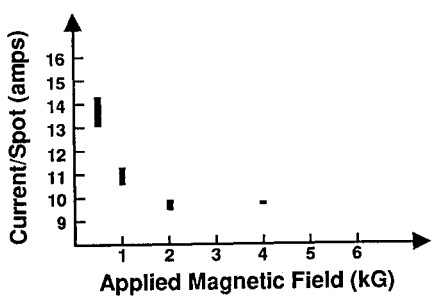

Fig. 10. Plot of calculated current per emission site during the first 300 ns of current pulse versus applied B-field.

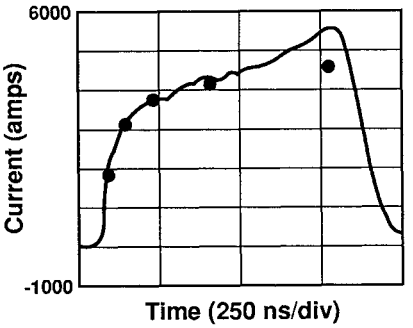

Fig. 11. Plot showing current waveform for a planar velvet cathode at an applied B-field of 2 kG. Solid points are the product of the number of observed emission sites and a value of 10 amps/site.

Acknowledgments

The authors gratefully acknowledge the efforts of J. Umphres and M. Engelhardt of LANL group CLS-7 for experimental support on the EGTF, and B. Carpenter of LANL group P-4 for photographic support. This work was supported by the United States Department of Energy through the University of California under contract LU-7405-ENG-36.

References

[1] L.A. Rosocha and K.B. Riepe, "Electron-Beam Sources For Pumping Large Aperture KrF Lasers," Fusion Technology, 11, 576 (1987).

[2] Science Research Laboratory Inc., "Investigation of Cold Cathode Diode Behavior on the Electron Gun Test Facility," Report #SRL-07-F-1987, unpublished.

[3] G.A. Mesyats and D.I. Proskurovsky, *Pulsed Electrical Discharge in Vacuum* (Springer-Verlag, Berlin Heidelberg 1989).

[4] R.K. Parker, R.E. Anderson, and C.V. Duncan, "Plasma Induced Field Emission and the Characteristics of High Current Electron Flow," J. Appl. Phys., 45, 2463 (1974).

[5] L.A. Rosocha, G.R. Allen, J.J. Coogan, C.R. Mansfield, E.A. Rose, and R.P. Shurter, "Electron Beam Pumping Technology Development for High Energy KrF Lasers," in *LASERS '90* (1990).

[6] T.Y. Chang, "Improved Uniform-Field Electrode Profiles for TEA Laser and High Voltage Applications," Rev. Sci.Instrum., 44, 405 (1973).

[7] Hain Oona, "Effects of High B-Fields on Current Localization and Closure Velocity," Los Alamos National Laboratory internal memo CLS-7:90-078, unpublished (1990).

[8] J.E. Eninger, "Broad Area Electron Beam Technology for High Power Gas Lasers," *Dig. Tech. Papers, 3rd IEEE Pulse Power Conf.*, p. 499 (1981).

[9] D. Hinshelwood, "Explosive Emission Cathode Plasmas in Relativistic Electron Beam Diodes," NRL-5492, Naval Research Laboratory (1985).

[10] Y.Y. Lau, "Effects of Surface Roughness on the Quality of Electron Beams," J. Appl. Phys., 61, 36 (1987).

[11] R.L. Boxman, S. Goldsmith, I. Izraeli, and S. Shalev, "A Model of the Multicathode-Spot Vacuum Arc," IEEE Transactions on Plasma Science, PS-11, 138 (1983).

[12] B. Hiller and R. Hanson, "Simultaneous Planar Measurements of Velocity and Pressure Fields in Gas Flows Using Laser-Induced Fluorescence," Applied Optics, 27, 33 (1987).

[13] S. Ya. Melomyttsev, S.D. Korovin and G.A. Mesyats, "Screening Effect in High-Current Diodes," Sov. Tech. Phys. Lett., 6, 466 (1980).